J. Am. Chem. Soc. 1988, 110, 7084-7092

Trinuclear, Mixed Pt_2Pd–1-Methyluracil and –1-Methylthymine Blues with +2.33 Average Metal Oxidation State: Preparation, Crystal Structures, and Solution Studies

Wolfgang Micklitz,[1a] Gerhard Müller,[1b] Brigitte Huber,[1b] Jürgen Riede,[1b] Farouk Rashwan,[1c] Jürgen Heinze,[1c] and Bernhard Lippert*,[1a]

Contribution from the Institut für Anorganische und Analytische Chemie, Universität Freiburg, D-7800 Freiburg, Federal Republic of Germany, the Institut für Physikalische Chemie, Universität Freiburg, D-7800 Freiburg, Federal Republic of Germany, and the Anorganisch-Chemisches Institut der Technischen Universität München, D-8046 Garching, Federal Republic of Germany. *Received March 22, 1988*

Abstract: Trinuclear, mixed Pt_2Pd complexes of composition *cis*-$[A_2PtL_2PdL_2PtA_2]X_2$ ($[Pt_2Pd]^{2+}$, **3**) and *cis*-$[A_2PtL_2PdL_2PtA_2]X_3$ ($[Pt_2Pd]^{3+}$, **5**), containing bridging 1-methyluracilato (1-MeU, $C_5H_5N_2O_2$) and 1-methylthyminato (1-MeT, $C_6H_7N_2O_2$) ligands L in mutual head–head orientation, different amine ligands A_2 ($2NH_3$, en), and different counterions X (NO_3^-, ClO_4^-), have been synthesized and characterized by several methods, including X-ray analysis. In **3**, all three metals are in the +II oxidation state, and the compounds are golden-tan. In **5**, one of the three metals is +III, and the compounds display a purple-blue metallic shine in the solid state. Compounds studied by X-ray crystallography were $[A_2PtL_2PdL_2PtA_2](ClO_4)_2\cdot2.25H_2O$ (A = NH_3, L = 1-MeU), **3a**, $[A_2PtL_2PdL_2PtA_2](NO_3)_3\cdot HNO_3\cdot5H_2O$ (A = NH_3, L = 1-MeU), **5a**, $[A_2PtL_2PdL_2PtA_2](NO_3)_3\cdot11H_2O$ (A = NH_3, L = 1-MeU), **5b**, and $[A_2PtL_2PdL_2PtA_2](NO_3)_3\cdot12H_2O$ (A_2 = en, L = 1-MeT), **5g**. All four compounds crystallize in the triclinic system, space group $P\bar{1}$. Cell dimensions are a = 12.064 (2) Å (**3a**), 10.032 (2) Å (**5a**), 11.611 (4) Å (**5b**), 10.270 (1) Å (**5g**), b = 12.524 (1) Å, 10.160 (2) Å, 10.083 (2) Å, 11.627 (1) Å, c = 13.730 (1) Å, 11.666 (2) Å, 12.121 (4) Å, 12.274 (1) Å, α = 80.05 (1)°, 103.33 (1)°, 109.19 (2)°, 105.23 (1)°, β = 106.70 (1)°, 106.29 (1)°, 106.29 (2)°, 102.87 (1)°, γ = 108.62 (1)°, 96.03 (1)°, 99.73 (2)°, 105.72 (1)°, V = 1875.4 Å^3, 1092.1 Å^3, 1231.8 Å^3, 1291.3 Å^3, Z = 2 (**3a**), 1 (**5a**, **5b**, **5g**). The cations of all compounds are centrosymmetric with Pd sitting in the center. Pt coordination in all cases is through N3 of the L ligand and Pd coordination through the exocyclic O4. Pt··Pd distances are 2.839 (1) and 2.837 (1) Å in the two crystallographically independent cations of **3a** and 2.634 (1) (**5a**), 2.641 (1) (**5b**), and 2.646 (1) Å (**5g**). The Pd–O(4) distances also undergo a significant shortening in **5** as compared to **3a**. The formation of **5** from **3** was monitored both by oxidative titration with Ce^{IV} and by visible spectroscopy (main absorption at 608–610 nm, $\epsilon \simeq$ 11 000). Complexes **5** are paramagnetic (Evans method), consistent with the presence of one unpaired electron per trinuclear unit. Cyclic voltammetry, performed in propylenecarbonate, indicates the existence of four redox states $[Pt_2Pd]^{n+}$ with n = 1, 2, 3, and 4. $E°$ values (versus Ag/AgCl) are −0.425, +0.68, and +1.34 V for the respective pairs.

The successful crystallization and structure determination of *cis*-diammineplatinum α-pyridone blue in 1977[2] and the more recent findings that the ethylenediamineplatinum analogue[3] as well as the *cis*-diammineplatinum 1-methyluracil blue[4] have similar structures have substantially contributed to the understanding of "platinum blues". Interest in the "blues" comes both from their challenging chemistry and their antitumor properties.[5] All three structurally characterized "blues" are tetranuclear species, comprised of two dinuclear *cis*-$[X_2PtL_2PtX_2]$ subunits, each of which contains two bridging ligands (L = deprotonated α-pyridone and 1-methyluracil, 1-MeU) in a head–head orientation (I in Chart I). Formally, the Pt_4 chain consists of 3 Pt^{II} and 1 Pt^{III} but since the unpaired electron is delocalized over all four Pt atoms,[6] description as a $[Pt(2.25)]_4$ species is justified. This situation also applies to tetranuclear "blues" derived from mixed amine complexes of type *xis*-$[X_2PtL_2PtY_2]^{2+}$ (X_2 = $(NH_3)_2$, Y_2 = bipy).[7] Oxidation of the diplatinum(II) precursor to the Pt(2.25) "blue" is conveniently achieved by use of HNO_3/O_2 or $HClO_4/O_2$ but also brought about by metal ions such as Ag^+, Fe^{3+}, and Ce^{4+}.[8]

Considering the solution chemistry of *cis*-diammineplatinum 1-methyluracil blue, it is quite clear that the Pt(2.25) blue, $[(NH_3)_2Pt(1\text{-MeU})_2Pt(NH_3)_2]_2^{5+}$, is *a* "blue" rather than *the* blue in this system. When dissolved in water, the blue-green color due to a strong absorption at 740 nm fades away rather quickly,[8] whereas blue species absorbing in the 550–650-nm range are quite stable. For this reason, we have been interested in 1-MeU bridged Pt complexes with structural features different from those found in the dimer-of-dimer type "blue". Encouraged by our finding of an unexpectedly facile displacement of two NH_3 ligands from a 1-MeU bridged diplatinum(III) complex,[9] we have tried to synthesize trinuclear Pt complexes of type II (Chart I), containing four 1-MeU bridges. While these attempts have not been fully successful as yet, we were able to prepare the mixed Pt_2Pd analogue III in two different oxidation states, $Pt^{II}{}_2Pd^{II}$ and (formally) $Pt^{II}{}_2Pd^{III}$, with the possibility to vary the amine ligands ($(NH_3)_2$ and ethylenediamine, en) and the bridging nucleobase (1-MeU

Chart I

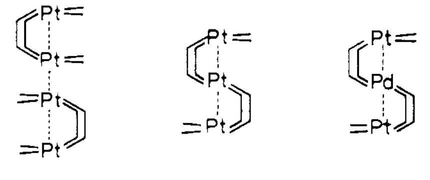

I II III

---

* Author to whom correspondence should be addressed at University of Dortmund, Department of Chemistry, Otto-Hahn-Strasse, 4600 Dortmund, Federal Republic of Germany.

(1) (a) Institut für Anorganische und Analytische Chemie, Universität Freiburg. (b) Technische Universität München. (c) Institut für Physikalische Chemie, Universität Freiburg.

(2) (a) Barton, J. K.; Rabinowitz, H. N.; Szalda, D. J.; Lippard, S. J. *J. Am. Chem. Soc.* **1977**, *99*, 2827. (b) Barton, J. K.; Szalda, D. J.; Rabinowitz, H. N.; Waszczak, J. V.; Lippard, S. J. *J. Am. Chem. Soc.* **1979**, *101*, 1434.

(3) O'Halloran, T. V.; Roberts, M. M.; Lippard, S. J. *J. Am. Chem. Soc.* **1984**, *106*, 6427.

(4) Mascharak, P. K.; Williams, I. D.; Lippard, S. J. *J. Am. Chem. Soc.* **1984**, *106*, 6428.

(5) Davidson, J. P.; Faber, P. J.; Fischer, R. G.; Mansy, S.; Peresie, H. J.; Rosenberg, B.; Van Camp, L. *Cancer Chemother. Rep., Part 1* **1975**, *59*, 287.

(6) O'Halloran, T. O.; Mascharak, P. K.; Williams, I. D.; Roberts, M. M.; Lippard, S. J. *Inorg. Chem.* **1987**, *26*, 1261.

(7) Micklitz, W.; Trötscher, G.; Lippert, B., to be submitted for publication.

(8) Lippert, B.; Schöllhorn, H.; Thewalt, U. *Inorg. Chem.* **1987**, *26*, 1736.

(9) Lippert, B.; Schöllhorn, H.; Thewalt, U. *Inorg. Chem.* **1986**, *25*, 407.

0002-7863/88/1510-7084$01.50/0

and 1-methylthymine, 1-MeT).

A preliminary report on these findings has appeared.[10]

Experimental Section

Preparation of Compounds. *cis*-$(NH_3)_2PtCl_2$,[11] en$PtCl_2$,[12] (bipy)-$PtCl_2$,[13] solutions of $[Pd(H_2O)_4](NO_3)_2$[14] and $[Pd(H_2O)_4](ClO_4)_2$,[15] *cis*-$(NH_3)_2Pt(1\text{-}MeU)_2\cdot 4H_2O$, **1a**,[16] *cis*-$(NH_3)_2Pt(1\text{-}MeT)_2\cdot 2.5H_2O$, **1b**,[17] (en)$Pt(1\text{-}MeU)_2\cdot 5H_2O$, **1c**,[18] *cis*-$[(NH_3)_2Pt(1\text{-}MeU)_2Pd(en)](NO_3)_2\cdot(H_2O)_n$ ($n = 0$–6), **4a**,[18] and $[(en)Pt(1\text{-}MeU)_2Pd(en)]SO_4\cdot 3H_2O$, **4b**,[18] were prepared as described.

(en)$Pt(1\text{-}MeT)_2\cdot 5H_2O$, **1d**, was obtained in a similar way as **1a–c** through reaction of $[(en)Pt(H_2O)_2]^{2+}$ and 1-MeT, subsequent purification via sephadex (G-10-120) chromatography, and slow evaporation. Colorless microcrystals, yield 35%. Anal. Calcd for $(C_2H_8N_2)Pt(C_6H_7N_2O_2)_2\cdot 5H_2O$: C, 26.70; H, 5.12; N, 13.35; O, 22.86. Found: C, 26.81; H, 5.21; N, 13.49; O, 22.63.

cis-$(NH_3)_2Pt(1\text{-}MeU)_2PdCl_2$, **2**, was prepared by mixing an aqueous solution of **1a** (0.5 mmol in 15 mL of H_2O) and solid K_2PdCl_4 (0.5 mmol). **2** started to precipitate almost immediately. After 1 h of stirring, the precipitate was filtered off and washed with cold water first, then with acetone, and ether. Grayish-tan precipitate, yield 70%. Anal. Calcd for $(NH_3)_2Pt(C_5H_5N_2O_2)_2PdCl_2$: C, 18.29; H, 2.46; N, 12.80; Cl, 10.80. Found: C, 18.19; H, 2.37; N, 12.66; Cl, 10.87.

cis-$[(NH_3)_2Pt(1\text{-}MeU)_2Pd(1\text{-}MeU)_2Pt(NH_3)_2](ClO_4)_2\cdot 2.25H_2O$, **3a**, was prepared by mixing an aqueous solution of **1a** (0.5 mmol in 20 mL of N_2-saturated H_2O) with 0.25 mmol of $[Pd(OH_2)_4](ClO_4)_2$ (dissolved in 6 mL of 1 M $HClO_4$) and stirring the solution under an atmosphere of N_2 for 1 h at 22 °C. A golden-tan precipitate (yield 80%) of **3a** was filtered, then washed with water, methanol, and ether, and recrystallized from water (70 °C). Single crystals, suitable for X-ray diffraction, were obtained this way. Anal. Calcd for $[(NH_3)_2Pt(C_5H_5N_2O_2)_2Pd(C_5H_5N_2O_2)_2Pt(NH_3)_2](ClO_4)_2\cdot 2.25H_2O$: C, 18.41; H, 2.83; N, 12.88; O, 22.38; Cl, 5.43. Found: C, 18.38; H, 2.76; N, 12.82; O, 22.60; Cl, 5.45.

cis-$[(NH_3)_2Pt(1\text{-}MeU)_2Pd(1\text{-}MeU)_2Pt(NH_3)_2](NO_3)_2\cdot 5.5H_2O$, **3b**, was prepared by reacting an aqueous suspension of **2** (0.35 mmol in 50 mL N_2-saturated water) with $AgNO_3$ (0.7 mmol, 4 h at 22 °C, N_2, filtration of AgCl) and then adding **1a** (0.5 mmol) and $NaNO_3$ (0.9 mmol). A golden-tan precipitate of **3b** was collected and washed with methanol and ether (yield 52%). Anal. Calcd for $C_{20}H_{43}N_{14}O_{19.5}Pt_2Pd$: C, 18.65; H, 3.36; N, 15.22; O, 24.22. Found: C, 18.66; H, 3.34; N, 15.21; O, 24.24.

$[(en)Pt(1\text{-}MeU)_2Pd(1\text{-}MeU)_2Pt(en)](ClO_4)_2\cdot 2H_2O$, **3c**, and *cis*-$[(NH_3)_2Pt(1\text{-}MeT)_2Pd(1\text{-}MeT)_2Pt(NH_3)_2](ClO_4)_2$, **3d**, were prepared in analogy to **3a**. Golden-tan precipitates of **3c** (yield 81%) and **3d** (yield 44%) were filtered off, washed with water, methanol, and ether, and then recrystallized from water (70 °C). Anal. Calcd for $C_{24}H_{40}N_{12}O_{18}Pt_2PdCl_2$, **3c**: C, 21.32; H, 2.98; N, 12.43; O, 21.30; Pt + Pd, 36.7; Cl, 5.24. Found: C, 21.26; H, 3.02; N, 12.39; Pt + Pd, 37.2, Cl, 4.98. Anal. Calcd for $C_{24}H_{40}N_{12}O_{16}Pt_2PdCl_2$, **3d**: C, 21.84; H, 3.05; N, 12.73; Cl, 5.37. Found: C, 21.80; H, 3.08; N, 12.55; Cl, 5.68.

Oxidation of Trinuclear $Pt^{II}_2Pd^{II}$ Compounds. As outlined below (Results and Discussion), formation of $Pt^{II}_2Pd^{III}$ complexes can take place via different routes. Yields of the isolated products varied from 2–60% for the different procedures. No attempts were made to optimize yields. The various complexes were obtained either through oxidation of a $Pt^{II}_2Pd^{II}$ precursor (compounds **3**) by HNO_3 ($[(NH_3)_2Pt(1\text{-}MeU)_2Pd(1\text{-}MeU)_2Pt(NH_3)_2](NO_3)_3\cdot HNO_3\cdot 5H_2O$, **5a**, $[(NH_3)_2Pt(1\text{-}MeU)_2Pd(1\text{-}MeU)_2Pt(NH_3)_2](NO_3)_3\cdot 11H_2O$, **5b**), through oxidation by Cl_2 ($[(NH_3)_2Pt(1\text{-}MeU)_2Pd(1\text{-}MeU)_2Pt(NH_3)_2](ClO_4)_3\cdot 6H_2O$, **5d**), through condensation of *cis*-A_2PtL_2 (A = NH_3 or (en)/2; L = 1-MeU or 1-MeT) and $[Pd(H_2O)_4]^{2+}$ under oxidative conditions (HNO_3) without isolation of the precursor **3** ($[(NH_3)_2Pt(1\text{-}MeU)_2Pd(1\text{-}MeU)_2Pt(NH_3)_2](NO_3)_3\cdot 5H_2O$, **5c**, $[(NH_3)_2Pt(1\text{-}MeT)_2Pd(1\text{-}MeT)_2Pt(NH_3)_2](NO_3)_3\cdot 5H_2O$, **5f**, $[(en)Pt(1\text{-}MeT)_2Pd(1\text{-}MeT)_2Pt(en)](NO_3)_3\cdot 12H_2O$, **5g**), or from a dinuclear $Pt^{II}Pd^{II}$ precursor (**4b**) on HNO_3 treatment ($[(en)Pt(1\text{-}MeU)_2Pd(1\text{-}MeU)_2Pt(en)](NO_3)_3\cdot HNO_3\cdot 6H_2O$, **5e**). The specific conditions leading to the isolation of **5a–d** have been described.[10] **5e** was obtained as follows: To a solution of **4b** (2 mmol in 10 mL of water) was added 10 mL of concentrated HNO_3 and the solution was kept in an open flask at room temperature with stirring. During this time, the color of the sample changed from orange via green to blue. After addition of 80 mL of water and slow evaporation at 3 °C, **5e** crystallized as purple-blue cubes with a metallic luster (11% yield). Compounds **5f** and **5g** were obtained from **1b** and **1d** (0.5 mmol in 20 mL of water), to which a solution of $[Pd(H_2O)_4](NO_3)_2$ (0.25 mmol, 1.3 N HNO_3) had been added. The originally colorless solution became deep red and then dark blue. A small amount of an unidentified red product was filtered off, and then the solution was allowed to slowly evaporate at 3 °C. Yields of the compounds were 22% in both cases.

Anal. Calcd for $C_{20}H_{43}N_{16}O_{25}Pt_2Pd$, **5a**: C, 17.11; H, 3.09; N, 15.96; O, 28.49; Pt + Pd, 35.36. Found: C, 17.06; H, 2.90; N, 16.28; O, 37.37; Pt + Pd 35.0 Formulation as a tetrahydrate would fit elemental analysis better for oxygen, but results of X-ray analysis favor the presence of 5 water molecules. As with related compounds,[10] gradual loss of water appears possible.

Anal. Calcd for $C_{20}H_{42}N_{15}O_{22}Pt_2Pd$, **5c**: C, 17.91; H, 3.16; N, 15.67; O, 26.24. Found: C, 18.02; H, 3.18; N, 15.69; O, 26.07.

Anal. Calcd for $C_{20}H_{44}N_{12}O_{26}Cl_3Pt_2Pd$, **5d**: C, 16.32; H, 3.01; N, 11.42; O, 28.27; Cl, 7.23. Found: C, 16.30; H, 2.99; N, 11.24; O, 28.43; Cl, 7.50.

Anal. Calcd for $C_{24}H_{49}N_{16}O_{26}Pt_2Pd$, **5e**: C, 19.55; H, 3.35; N, 15.20; O, 28.21; Pt + Pd, 28.21. Found: C, 19.45; H, 3.50; N, 15.42; O, 28.13; Pt + Pd, 33.7.

Anal. Calcd for $C_{24}H_{50}N_{15}O_{22}Pt_2Pd$, **5f**: C, 20.63; H, 3.61; N, 15.04; O, 25.20. Found: C, 20.59; H, 3.72; N, 15.16; O, 25.40.

Anal. Calcd for $C_{28}H_{68}N_{15}O_{29}Pt_2Pd$, **5g**: C, 21.34; H, 4.35; N, 13.34; O, 29.45. Found: C, 21.35; H, 4.44; N, 13.47; O, 29.21.

Crystal Structure Determinations of 3a, 5a, 5b, and 5g. Suitable single crystals were sealed under an atmosphere of argon into glass capillaries and examined directly on the diffractometer. Triclinic cell symmetry was found for all compounds. Reduced-cell calculations did not indicate any higher symmetry. As space group $P\bar{1}$ (no. 2) was initially assumed and confirmed by the successful refinement of the structures. The cations of all four compounds closely adhere to crystallographic centrosymmetry, with the Pd atoms being situated on the inversion centers. In the structure of **3a**, there are two crystallographic independent cations, thus resulting in $Z = 2$. Table I summarizes the cell constants and important numbers pertinent to data collection and structure refinement.

Intensity Data Collection. The integrated intensities were collected with graphite-monochromatized Mo Kα radiation (λ = 0.71069 Å) and corrected for decay and Lorentz-polarization effects as well as for absorption. For the latter correction scans at intervals of 10° around the diffraction vectors of 7–10 selected reflections near χ = 90° served to determine the relative transmissions.

Structure Solution. The structures of **5a** and **5b** were solved by standard Patterson methods with SHELX-76.[19] Automated Patterson methods were used for **3a** and **5g** (SHELXS-86).[20]

Refinement. The cations were generally refined with anisotropic displacement parameters. Severe disorder and/or partial occupancy was found for several of the anions and for most of the cocrystallized water molecules. Actually, the final difference maps of all four structures showed peaks which might be attributed to additional partially occupied water molecule positions. Attempts to refine these sites failed, however. Therefore, the formula weights, calculated densities, and absorption coefficients listed in Table I are based only on those atoms, which could be refined successfully.

In the structure of **3a**, one ClO_4^- anion was refined with anisotropic displacement parameters for the Cl atom and isotropic ones for the O atoms, which were distributed over three alternative sites (occupancy ratio 0.5/0.25/0.25). The other ClO_4^- anion was found to be disordered as two half-occupied tetrahedra sharing two common O atoms (all atoms isotropic). Bond length constraints were applied to the Cl–O and O··O distances (1.43 (1) and 2.34 (1) Å, respectively). All H atoms were neglected.

For **5a**, one NO_3^- anion was refined anisotropically (full occupancy). For the second one, a disordered model was used with two alternative sites (50/50) for each O atom. Again, bond length constraints were applied (N–O, 1.22 (1); O··O, 2.11 (1) Å). This second NO_3^- anion was found to be close to its symmetry-equivalent with a geometry not unlike that of hydrogen-bonded $[O_2NO\text{-}H\text{-}ONO_2]^-$ dimers,[21] with an angle of

---

[10] Micklitz, W.; Müller, G.; Riede, J.; Lippert, B. *J. Chem. Soc., Chem. Commun.* **1987**, 76.

[11] (a) Dhara, S. C. *Indian J. Chem.* **1970**, *8*, 143. (b) Raudaschl, G.; Lippert, B.; Hoeschele, J. D.; Howard-Lock, H. E.; Lock, C. J. L.; Pilon, P. *Inorg. Chim. Acta* **1985**, *106*, 141.

[12] Johnson, G. L. *Inorg. Synth.* **1966**, *8*, 242.

[13] Morgan, G. T.; Burstall, F. H. *J. Chem. Soc.* **1934**, 965.

[14] Elding, L. I., personal communication.

[15] Elding, L. I. *Inorg. Chim. Acta* **1972**, *6*, 647.

[16] Neugebauer, D.; Lippert, B. *J. Am. Chem. Soc.* **1982**, *104*, 6596.

[17] Lippert, B.; Neugebauer, D. *Inorg. Chim. Acta* **1980**, *46*, 171.

[18] Micklitz, W.; Riede, J.; Huber, B.; Müller, G.; Lippert, B. *Inorg. Chem.* **1988**, *27*, 1979.

[19] Sheldrick, G. M. *SHELX-76, Program for Crystal Structure Determination*; University of Cambridge: Cambridge, England, 1976.

[20] Sheldrick, G. M. In *Crystallographic Computing 3*; Sheldrick, G. M., Krüger, C., Goddard, R., Eds.; Oxford University Press: Oxford, 1985; p 175.

[21] See, e.g., Emsley, J. *Chem. Soc. Rev.* **1980**, *9*, 91 and references cited.

Table I. Crystal Data and Experimental Details of Structure Determinations of **3a**, **5a**, **5b**, and **5g**

compound	**3a**	**5a**	**5b**	**5g**
formula	$C_{20}H_{32}N_{12}O_{16}Cl_2PdPt_2\cdot 2.25H_2O$	$C_{20}H_{32}N_{15}O_{17}PdPt_2\cdot HNO_3\cdot 5H_2O$	$C_{20}H_{32}N_{15}O_{17}PdPt_2\cdot 11H_2O$	$C_{28}H_{44}N_{15}O_{17}PdPt_2\cdot 12H_2O$
fw	1304.21	1403.88	1448.96	1575.16
crystal system	triclinic	triclinic	triclinic	triclinic
space group	$P\bar{1}$	$P\bar{1}$	$P\bar{1}$	$P\bar{1}$
a, Å	12.064 (2)	10.032 (2)	11.611 (4)	10.270 (1)
b, Å	12.524 (1)	10.160 (2)	10.083 (2)	11.627 (1)
c, Å	13.730 (1)	11.666 (2)	12.121 (4)	12.274 (1)
α, deg	80.05 (1)	103.33 (1)	109.19 (2)	105.23 (1)
β, deg	106.70 (1)	106.29 (1)	106.29 (2)	102.87 (1)
γ, deg	108.62 (1)	96.03 (1)	99.73 (2)	105.72 (1)
V, Å^3	1875.4	1092.1	1231.8	1291.3
Z	2	1	1	1
d_{calcd}, g cm^{-3}	2.309	2.134	1.953	2.025
d_{measd}, g cm^{-3}	2.30	2.14		1.98
cryst size, mm	0.15•0.15•0.35	0.15•0.30•0.50	0.30•0.25•0.40	0.28•0.33•0.40
μ (Mo Kα), cm^{-1}	82.2	69.6	61.7	59.0
F(000), e	1245	677	705	775
diffractometer	Enraf-Nonius CAD4	Syntex P2$_1$	Syntex P2$_1$	Syntex P2$_1$
T, °C	22	−35	−40	22
scan type	$\vartheta - 2\vartheta$	ω	ω	ω
scan width, deg in ω	$0.8 + 0.35 \tan \vartheta$	0.8	1.0	1.0
hkl range	+15,±16,±17	+12,±12,±14	+14,±12,±14	+12,±13,±14
$(\sin \vartheta/\lambda)_{max}$, Å^{-1}	0.639	0.639	0.617	0.595
standards	$3\bar{5}3$, $70\bar{7}$, $\bar{1}\bar{5}\bar{3}$	200, 020, 033	300, 002, 020	040, 400, 004
no. of measd reflcns	8167	4748	4846	4553
no. of unique reflcns	8144	4748	4846	4553
R_{int}	0.02			
no. of reflcns used in calculatns ($F_o \geq 4\sigma(F_o)$)	5614	4448	4240	4134
rel transmission	0.68–1.00	0.36–1.00	0.63–1.00	0.61–1.00
param ref	504	324	275	312
R^a	0.035	0.042	0.045	0.029
$R_w{}^b$	0.036	0.057	0.052	0.035
highest peak in final diff map, eÅ^{-3}	0.95	1.75	2.93	1.06

[a] $R = \sum(||F_o| - |F_c||)/\sum|F_o|$. [b] $R_w = [\sum w(|F_o| - |F_c|)^2/\sum wF_o^2]^{1/2}$, $w = 1/\sigma^2(F_o)$; function minimized: $\sum w(|F_o| - |F_c|)^2$.

65.4° between the two NO_3^- planes. Although the missing H atom at 0.5, 0.5, 0.0 could not be located in difference maps, it seems plausible that the overall composition therefore amounts to the presence of three NO_3^- counterions and one cocrystallized HNO_3 molecule per cation. H atoms were ignored.

For **5b**, the nitrate anions were refined isotropically as rigid groups with an occupancy ratio of 0.6/0.5/0.4, equivalent to the presence of three anions per cation. H atoms were neglected.

For **5g**, one of the nitrate anions was found to be ordered and could be refined anisotropically. The second one was located on an inversion center and was modeled as two sets of three O atoms with a quarter occupancy at a common N atom (constraints, N–O, 1.220 (5), O··O, 2.110 (5) Å). Again, this amounts to the presence of three counterions per cation. In analogy to the 1-MeU complexes **3a**, **5a**, and **5b**, the 1-MeT ligands were assumed to be metal-coordinated via their N3 and O4 atoms. This assignment is substantiated by the uniform displacement parameters for the atoms C5 and N1 (cf. also discussion in ref 22). Ten hydrogen atoms out of a total of 22 could be located in difference maps. The remainder was calculated at idealized geometrical positions. Thereby, found H atoms served to determine the conformations of the methyl groups. The H atoms were held constant in the final refinement cycles (U_{iso} = 0.055 Å^2).

For the refinement SHELX-76 was applied.[19] Further details of the procedures used in data collection and structure refinement have been described elsewhere.[23] Tables II–V contain the atomic coordinates and equivalent isotropic displacement parameters.

Electrochemistry. The electrochemical experiments with **5a** were run in propylenecarbonate (PC) with 0.1 M tetra-*n*-butylammonium hexafluorophosphate (Fluka, recrystallized from 1:2 water/MeOH and dried in vacuo at 120 °C prior to use) as supporting electrolyte. Technical PC was dried with sodium and then distilled under vacuum. Only the middle fraction was used in the experiments.

All voltammetric experiments were carried out in a standard three-electrode cell under argon. The cell was equipped with an integrated alumina column to dry the solvent system. The working electrode was a Pt disk (1.39 mm diameter) sealed in soft glass. A Pt wire, wrapped around the glass of the working electrode, was used as the counter electrode, and an Ag/AgCl element, immersed in PC, was used as the pseudo reference electrode. Potentials were calibrated with ferrocene.

The cyclovoltammetric measurements were performed with a PAR Model 174 potentiostat and a VSG 72 voltage scan generator (Bank, Göttingen, FRG). For AC-voltammetry, in addition a PAR Model 372 interface, an Ithaco Model 393 lock-amplifier (Ithaco Inc., Ithaca, NY), and a Hewlett-Packard Model 4204 A oscillator (Hewlett-Packard Co, Palo Alto, CA) were used. Data were recorded on an X-Y recorder PM 8131 (Phillips GmbH, Kassel, FRG).

Other Measurements. ^{1}H NMR, vibrational, and UV spectra were recorded, and oxidative titrations by means of $Ce(SO_4)_2$ were carried out as described elsewhere.[18] pH titrations were performed both by use of standard glass electrodes and pH meters (Metrohm, Switzerland) and an automated E 536 potentiograph (Metrohm) in an atmosphere of nitrogen.

Results and Discussion

$[Pt_2Pd]^{2+}$ (3). Preparation of the perchlorate salt of $[Pt_2Pd]^{2+}$ followed the general route applied to prepare other heteronuclear Pt_2M complexes,[16,17,24-27] namely

$$\underset{\mathbf{1a}}{2\textit{cis}\text{-}(NH_3)_2PtL_2} + [Pd(H_2O)_4](ClO_4)_2 \rightarrow \underset{\mathbf{3a}}{[(NH_3)_2PtL_2PdL_2Pt(NH_3)_2](ClO_4)_2} + 4H_2O$$

The analogous nitrate salt could not be obtained this way because of rapid oxidation to $[Pt_2Pd]^{3+}$ (vide infra). It was, however,

---

(22) Schöllhorn, H.; Thewalt, U.; Lippert, B. *Inorg. Chim. Acta* **1984**, *93*, 19.

(23) Schmidbaur, H.; Schier, A.; Frazão, C. M. F.; Müller, G. *J. Am. Chem. Soc.* **1986**, *108*, 976.

(24) Lippert, B.; Schubert, U. *Inorg. Chim. Acta* **1981**, *56*, 15.

(25) Lippert, B.; Thewalt, U.; Schöllhorn, H.; Goodgame, D. M. L.; Rollins, R. W. *Inorg. Chem.* **1984**, *23*, 2807.

(26) Goodgame, D. M. L.; Rollins, R. W.; Lippert, B. *Polyhedron* **1985**, *4*, 829.

(27) Mutikainen, I.; Orama, O.; Pajunen, A.; Lippert, B. *Inorg. Chim. Acta* **1987**, *137*, 189.

Table II. Atomic Coordinates and Equivalent Isotropic Displacement Parameters of *cis*-$[(NH_3)_2Pt(1\text{-}MeU)_2Pd(1\text{-}MeU)_2Pt(NH_3)_2](ClO_4)_2 \cdot 2.25H_2O$ (**3a**)[a]

atom	x/a	y/b	z/c	U_{eq}	atom	x/a	y/b	z/c	U_{eq}
Pt1	0.1896 (1)	0.0298 (1)	0.1811 (1)	0.028	C412	0.6139 (9)	0.6697 (8)	0.3486 (6)	0.035
Pt2	0.4109 (1)	0.6900 (1)	0.4231 (1)	0.027	C512	0.7010 (10)	0.7047 (10)	0.2881 (8)	0.046
Pd1	0.0000	0.0000	0.0000	0.033	C612	0.7138 (10)	0.8052 (10)	0.2325 (8)	0.049
Pd2	0.5000	0.5000	0.5000	0.032	C122	0.1140 (10)	0.6391 (10)	0.0515 (9)	0.049
O211	0.2073 (6)	0.0981 (6)	0.3871 (6)	0.052	C222	0.2466 (8)	0.6417 (8)	0.2258 (8)	0.032
O411	−0.0613 (6)	0.0883 (6)	0.0734 (5)	0.040	C422	0.3010 (9)	0.4763 (8)	0.3132 (6)	0.036
O221	0.4163 (6)	0.2180 (6)	0.2428 (5)	0.043	C522	0.2231 (9)	0.4125 (9)	0.2292 (8)	0.038
O421	0.1100 (6)	0.1491 (6)	−0.0463 (5)	0.041	C622	0.1656 (9)	0.4673 (9)	0.1464 (8)	0.044
O212	0.5128 (6)	0.9110 (5)	0.3059 (6)	0.046	Cl1	0.4244 (2)	0.7608 (2)	−0.0049 (2)	0.050
O412	0.5999 (6)	0.5713 (6)	0.3982 (5)	0.041	O11	0.3694 (10)	0.8383 (9)	0.0156 (9)	0.058
O222	0.2504 (6)	0.7402 (5)	0.2235 (5)	0.042	O21	0.5377 (8)	0.8232 (11)	−0.0257 (11)	0.097
O422	0.3591 (6)	0.4258 (5)	0.3890 (5)	0.040	O31	0.4401 (11)	0.6815 (8)	0.0825 (6)	0.059
N101	0.3037 (6)	−0.0298 (6)	0.1335 (6)	0.037	O41	0.3465 (12)	0.7020 (11)	−0.0911 (8)	0.105
N201	0.1196 (8)	−0.1245 (6)	0.2560 (6)	0.046	O11A	0.3801 (18)	0.8204 (16)	0.0481 (16)	0.075
N111	0.0606 (8)	0.1861 (8)	0.3584 (6)	0.047	O21A	0.5494 (9)	0.8237 (13)	−0.0027 (15)	0.033
N311	0.0811 (6)	0.0955 (6)	0.2283 (6)	0.035	O31A	0.4215 (19)	0.6512 (9)	0.0441 (16)	0.066
N121	0.4021 (6)	0.3608 (6)	0.1197 (6)	0.034	O41A	0.3575 (18)	0.7551 (20)	−0.1088 (8)	0.100
N321	0.2538 (6)	0.1815 (6)	0.1049 (6)	0.028	O11B	0.3447 (17)	0.8280 (16)	−0.0110 (18)	0.057
N102	0.2692 (8)	0.6381 (6)	0.4919 (6)	0.044	O21B	0.5229 (16)	0.8262 (18)	−0.0453 (19)	0.088
N202	0.5147 (6)	0.7945 (6)	0.5364 (6)	0.042	O31B	0.4629 (24)	0.7197 (21)	0.0991 (9)	0.127
N112	0.6463 (6)	0.8744 (6)	0.2366 (6)	0.041	O41B	0.3556 (18)	0.6658 (13)	−0.0638 (17)	0.074
N312	0.5484 (6)	0.7387 (6)	0.3526 (6)	0.032	Cl2	−0.0634 (4)	0.5145 (4)	0.2843 (4)	0.048
N122	0.1767 (6)	0.5792 (6)	0.1428 (6)	0.036	Cl2A	−0.0503 (5)	0.5402 (5)	0.3204 (4)	0.065
N322	0.3096 (6)	0.5887 (6)	0.3094 (5)	0.028	O12	0.0387 (6)	0.4826 (6)	0.3520 (6)	0.125
C111	0.1076 (12)	0.2205 (13)	0.4653 (9)	0.055	O22	−0.1677 (6)	0.4676 (6)	0.3222 (6)	0.167
C211	0.1215 (9)	0.1255 (9)	0.3273 (8)	0.039	O32	−0.0342 (10)	0.6367 (6)	0.2752 (10)	0.078
C411	−0.0191 (8)	0.1202 (8)	0.1630 (8)	0.034	O42	−0.0844 (12)	0.4781 (12)	0.1862 (6)	0.098
C511	−0.0777 (9)	0.1862 (8)	0.1950 (8)	0.039	OA2	−0.0521 (13)	0.5917 (16)	0.2174 (9)	0.263
C611	−0.0363 (10)	0.2170 (9)	0.2910 (9)	0.046	OC2	−0.0195 (13)	0.6292 (12)	0.3854 (15)	0.200
C121	0.5118 (9)	0.4381 (8)	0.1830 (9)	0.045	OH1	0.3372 (15)	0.7970 (15)	0.6807 (13)	0.105
C221	0.3611 (9)	0.2517 (6)	0.1603 (6)	0.032	OH2	0.3738 (11)	0.9660 (10)	0.4104 (10)	0.045
C421	0.1990 (8)	0.2158 (8)	0.0087 (6)	0.032	OH3	0.2053 (26)	0.8735 (24)	0.5072 (22)	0.054
C521	0.2440 (9)	0.3281 (8)	−0.0339 (6)	0.038	OH4	0.1811 (32)	0.9181 (20)	0.5448 (27)	0.084
C621	0.3411 (10)	0.3985 (8)	0.0229 (8)	0.040	OH5	0.3508 (58)	0.8746 (55)	0.6161 (51)	0.233
C112	0.6532 (11)	0.9833 (9)	0.1713 (9)	0.052	OH6	0.3152 (21)	0.7489 (20)	0.6894 (18)	0.093
C212	0.5666 (9)	0.8447 (8)	0.2986 (8)	0.035					

[a] $U_{eq} = (U_1U_2U_3)^{1/3}$, where U_i are the eigenvalues of the U_{ij} matrix.

Table III. Atomic Coordinates and Equivalent Isotropic Displacement Parameters of *cis*-$[(NH_3)_2Pt(1\text{-}MeU)_2Pd(1\text{-}MeU)_2Pt(NH_3)_2](NO_3)_3 \cdot HNO_3 \cdot 5H_2O$ (**5a**)[a]

atom	x/a	y/b	z/c	U_{eq}	atom	x/a	y/b	z/c	U_{eq}
Pt	0.2535 (1)	0.0228 (1)	0.0332 (1)	0.017	C52	0.5591 (12)	0.3841 (11)	0.2602 (12)	0.041
Pd	0.5000	0.0000	0.0000	0.020	C62	0.4806 (11)	0.4546 (11)	0.3190 (11)	0.038
N10	0.2802 (6)	−0.0738 (8)	0.1719 (6)	0.025	N100	0.5258 (13)	0.1660 (11)	0.4895 (10)	0.050
N20	0.1410 (6)	−0.1560 (8)	−0.0948 (6)	0.026	O110	0.5434 (10)	0.0820 (10)	0.4010 (9)	0.061
O21	0.0243 (6)	0.1666 (6)	−0.0723 (6)	0.027	O120	0.4107 (13)	0.2037 (13)	0.4776 (10)	0.073
O41	0.4352 (6)	0.0762 (8)	−0.1418 (6)	0.036	O130	0.6179 (17)	0.2073 (12)	0.5878 (11)	0.083
N11	0.0970 (8)	0.2584 (9)	−0.2100 (8)	0.032	N200	0.3187 (9)	0.5546 (11)	0.0323 (8)	0.049
N31	0.2307 (6)	0.1208 (8)	−0.1029 (6)	0.024	O210	0.4005 (13)	0.6541 (12)	0.1147 (12)	0.046
C11	−0.0214 (11)	0.3337 (13)	−0.2244 (12)	0.040	O220	0.3713 (13)	0.4641 (13)	−0.0171 (21)	0.031
C21	0.1125 (8)	0.1813 (9)	−0.1261 (8)	0.023	O230	0.1998 (11)	0.5721 (17)	−0.0153 (15)	0.053
C41	0.3256 (10)	0.1324 (11)	−0.1645 (9)	0.032	O240	0.4138 (37)	0.4927 (36)	0.0170 (55)	0.213
C51	0.3008 (12)	0.2006 (13)	−0.2597 (12)	0.043	O250	0.2320 (25)	0.5016 (27)	0.0727 (27)	0.122
C61	0.1883 (12)	0.2645 (13)	−0.2790 (12)	0.045	O260	0.3239 (43)	0.6725 (23)	0.0290 (46)	0.206
O22	0.1652 (6)	0.2119 (6)	0.2189 (5)	0.029	OH1	0.1842 (19)	0.0272 (19)	0.4017 (16)	0.055
O42	0.5686 (6)	0.1896 (6)	0.1149 (6)	0.034	OH2	−0.1771 (18)	0.1636 (22)	0.3477 (16)	0.058
N12	0.3443 (8)	0.3965 (8)	0.3058 (6)	0.031	OH3	0.0685 (17)	0.0552 (17)	0.3636 (13)	0.044
N32	0.3613 (6)	0.2011 (8)	0.1603 (6)	0.024	OH4	−0.0504 (18)	0.1330 (18)	0.3664 (13)	0.048
C12	0.2608 (12)	0.4660 (13)	0.3755 (11)	0.044	OH5	0.9762 (25)	0.5956 (25)	0.4824 (21)	0.023
C22	0.2831 (9)	0.2673 (9)	0.2276 (6)	0.025	OH6	0.9253 (27)	0.4218 (27)	0.3959 (23)	0.036
C42	0.4952 (9)	0.2545 (9)	0.1745 (10)	0.030					

[a] U_{eq} same as in Table II.

prepared via an alternative route which involved a neutral, heteronuclear (Pt, Pd) intermediate **2**:

$$\underset{\mathbf{1a}}{cis\text{-}(NH_3)_2PtL_2} + K_2PdCl_4 \rightarrow \underset{\mathbf{2}}{cis\text{-}(NH_3)_2PtL_2PdCl_2} + 2KCl$$

Reaction of **2** with $AgNO_3$ in the presence of additional **1a** gave **3b**:

$$\underset{\mathbf{2}}{cis\text{-}(NH_3)_2PtL_2PdCl_2} + 2AgNO_3 + \underset{\mathbf{1a}}{cis\text{-}(NH_3)_2PtL_2} \rightarrow$$
$$\underset{\mathbf{3b}}{[(NH_3)_2PtL_2PdL_2Pt(NH_3)_2](NO_3)_2} + 2AgCl$$

The ^1H NMR spectra of **3** in D_2O are as expected in that the 1-MeU resonances occur downfield from those of *cis*-$(NH_3)_2Pt(1\text{-}MeU)_2$. In D_2O, pD 3, doublets (^3J = 7 Hz) of H6 and H5 protons of the 1-MeU ligands are observed at 7.44 and 5.77 ppm. N-CH_3 gives a singlet at 3.39 ppm. As compared to the head-head dimer *cis*-$[(NH_3)_2Pt(1\text{-}MeU)_2Pt(NH_3)_2]^{2+}$, the effect of Pd in shifting H5 clearly is smaller. This situation also applies to dinuclear PtPd complexes, e.g., *cis*-$[(NH_3)_2Pt(1\text{-}MeU)_2Pd(en)]^{2+}$, **4a**.[18] We attribute this fact to a weaker interaction of Pd^{II} with the O4 oxygens of the 1-MeU ligands as compared to Pt^{II}. Spectra of **3** always show a weak set of signals

Table IV. Atomic Coordinates and Equivalent Isotropic Displacement Parameters of *cis*-$[(NH_3)_2Pd(1\text{-}MeU)_2Pd(1\text{-}MeU)_2Pt(NH_3)_2](NO_3)_3\cdot 11H_2O$ (**5b**)[a]

atom	x/a	y/b	z/c	U_{eq}	atom	x/a	y/b	z/c	U_{eq}
Pt	0.4710 (1)	0.2517 (1)	0.4931 (1)	0.016	C52	0.1260 (9)	−0.0968 (10)	0.2662 (10)	0.026
Pd	0.5000	0.0000	0.5000	0.017	C62	0.0421 (9)	−0.0165 (12)	0.2448 (10)	0.030
N10	0.4218 (6)	0.3201 (9)	0.6478 (6)	0.022	N100	0.7825 (8)	−0.1517 (10)	−0.0589 (9)	0.058
N20	0.6513 (6)	0.3784 (8)	0.6038 (8)	0.024	O110	0.7532 (8)	−0.1321 (10)	0.0352 (9)	0.047
O21	0.4787 (6)	0.3815 (6)	0.3074 (6)	0.027	O120	0.8163 (8)	−0.2620 (10)	−0.1029 (9)	0.085
O41	0.5750 (6)	−0.0147 (6)	0.3694 (6)	0.024	O130	0.7548 (8)	−0.0784 (10)	−0.1221 (9)	0.088
N11	0.5542 (8)	0.2390 (8)	0.1741 (6)	0.025	N200	0.9145 (11)	−0.0953 (15)	0.4502 (13)	0.158
N31	0.5232 (6)	0.1859 (8)	0.3413 (6)	0.021	O210	0.8803 (11)	0.0054 (15)	0.4254 (13)	0.062
C11	0.5510 (12)	0.3358 (13)	0.1039 (11)	0.037	O220	0.8439 (11)	−0.2231 (15)	0.3932 (13)	0.058
C21	0.5161 (9)	0.2738 (10)	0.2742 (9)	0.023	O230	1.0265 (11)	−0.0734 (15)	0.5124 (13)	0.161
C41	0.5689 (9)	0.0693 (10)	0.3091 (9)	0.024	N300	0.7761 (16)	0.0698 (13)	−0.0449 (16)	0.105
C51	0.6102 (10)	0.0360 (12)	0.2061 (10)	0.032	O310	0.7635 (16)	0.1935 (13)	−0.0322 (16)	0.017
C61	0.6035 (11)	0.1224 (11)	0.1434 (10)	0.030	O320	0.8828 (16)	0.0564 (13)	−0.0054 (16)	0.113
O22	0.2427 (6)	0.3446 (6)	0.4189 (6)	0.027	O330	0.6826 (16)	−0.0336 (13)	−0.0741 (16)	0.137
O42	0.3306 (6)	−0.0910 (6)	0.3647 (6)	0.025	OH1	0.8047 (6)	0.4483 (9)	0.3870 (8)	0.045
N12	0.0835 (6)	0.1336 (9)	0.2985 (8)	0.025	OH2	0.8484 (6)	0.2753 (10)	0.5197 (8)	0.045
N32	0.2907 (6)	0.1301 (8)	0.3897 (8)	0.019	OH3	0.6562 (8)	0.3684 (10)	0.8492 (8)	0.047
C12	−0.0067 (10)	0.2184 (13)	0.2774 (12)	0.035	OH4	1.0573 (9)	0.4462 (10)	0.7347 (9)	0.058
C22	0.2073 (9)	0.2102 (11)	0.3709 (9)	0.022	OH5	0.9997 (10)	0.4030 (13)	0.0590 (11)	0.067
C42	0.2532 (8)	−0.0178 (10)	0.3429 (9)	0.022	OH6	0.7559 (15)	−0.3916 (18)	0.0728 (16)	0.052

[a] U_{eq} same as in Table II.

Table V. Atomic Coordinates and Equivalent Isotropic Displacement Parameters of $[(en)Pt(1\text{-}MeT)_2Pd(1\text{-}MeT)_2Pt(en)](NO_3)_3\cdot 12H_2O$ (**5g**)[a]

atom	x/a	y/b	z/c	U_{eq}	atom	x/a	y/b	z/c	U_{eq}
Pt	−0.2565 (1)	1.0021 (1)	0.0020 (1)	0.011	C42	−0.0907 (5)	0.9203 (5)	0.1837 (5)	0.016
Pd	0.0000	1.0000	0.0000	0.012	C52	−0.0688 (6)	0.8814 (5)	0.2841 (5)	0.018
O21	−0.3587 (4)	1.2197 (4)	0.0565 (4)	0.021	C521	0.0521 (6)	0.8335 (6)	0.3154 (6)	0.029
O41	0.0757 (4)	1.1715 (3)	0.1249 (3)	0.017	C62	−0.1564 (6)	0.8937 (5)	0.3504 (5)	0.021
O22	−0.3893 (4)	1.0080 (4)	0.1919 (4)	0.022	N50	0.0568 (6)	0.2528 (5)	0.4342 (5)	0.029
O42	−0.0039 (4)	0.9173 (4)	0.1228 (3)	0.016	O51	0.1315 (6)	0.1876 (5)	0.4070 (5)	0.045
N10	−0.3739 (5)	0.8177 (4)	−0.0984 (4)	0.017	O52	−0.0718 (5)	0.2130 (5)	0.3807 (5)	0.040
N20	−0.3164 (5)	1.0305 (4)	−0.1538 (4)	0.017	O53	0.1144 (6)	0.3575 (5)	0.5167 (4)	0.039
N11	−0.1650 (5)	1.3854 (4)	0.1858 (4)	0.019	N60	0.0000	0.5000	0.0000	0.042
N31	−0.1457 (5)	1.1898 (4)	0.0949 (4)	0.013	O61	0.0829 (13)	0.6097 (6)	0.0485 (19)	0.067
N12	−0.2648 (5)	0.9374 (4)	0.3199 (4)	0.019	O62	0.0402 (13)	0.4172 (10)	−0.0492 (13)	0.036
N32	−0.2021 (5)	0.9586 (4)	0.1517 (4)	0.013	O63	−0.1289 (5)	0.4802 (13)	−0.0251 (13)	0.031
C10	−0.4369 (6)	0.8026 (5)	−0.2266 (5)	0.021	O6A	0.1027 (13)	0.4723 (18)	−0.0130 (21)	0.067
C20	−0.3466 (6)	0.9106 (6)	−0.2544 (5)	0.021	O6B	−0.1202 (10)	0.4212 (17)	−0.0490 (29)	0.122
C11	−0.2553 (6)	1.4640 (6)	0.2027 (6)	0.024	O6C	0.0157 (20)	0.6075 (8)	0.0607 (15)	0.048
C21	−0.2312 (6)	1.2634 (5)	0.1096 (5)	0.016	OH1	0.3109 (5)	0.3775 (5)	0.0036 (4)	0.043
C41	−0.0027 (5)	1.2402 (5)	0.1456 (5)	0.015	OH2	0.3244 (6)	0.7371 (5)	0.2198 (5)	0.051
C51	0.0653 (6)	1.3687 (5)	0.2216 (5)	0.018	OH3	0.4169 (5)	0.7510 (5)	0.4617 (5)	0.049
C511	0.2242 (6)	1.4216 (6)	0.2787 (6)	0.025	OH4	0.5171 (5)	0.6198 (5)	0.1513 (5)	0.047
C61	−0.0214 (6)	1.4357 (5)	0.2399 (5)	0.019	OH5	0.4108 (6)	0.3811 (6)	0.6213 (5)	0.061
C12	−0.3509 (6)	0.9601 (6)	0.3997 (5)	0.022	OH6	0.2152 (6)	0.6254 (5)	0.5457 (5)	0.056
C22	−0.2906 (5)	0.9703 (5)	0.2204 (5)	0.016					

[a] U_{eq} same as in Table II.

(ca. 5–10% of **3** in 0.05 M solution, sample heated) due to *cis*-$(NH_3)_2Pt(1\text{-}MeU)_2$, **1a**, which suggests that in solution partial dissociation occurs according to

$$\underset{\mathbf{3b}}{[(NH_3)_2Pt(1\text{-}MeU)_2Pd(1\text{-}MeU)_2Pt(NH_3)_2]^{2+}} + 4H_2O \rightleftharpoons 2\underset{\mathbf{1a}}{[(NH_3)_2Pt(1\text{-}MeU)_2]} + [Pd(H_2O)_4]^{2+}$$

Unlike with the heterometal Zn^{II},[28] exchange between free and coordinated Pd^{II} is sufficiently slow to give individual resonances for **3** and **1**.

The UV spectrum of **3** is consistent with this interpretation: Under the conditions of the UV experiment ($6\cdot 10^{-5}$ M), **3** appears to be largely dissociated as judged by the weakness of the band at 282 nm (characteristic of N3,O4 metal binding of 1-MeU)[18] relative to that around 265 nm which is characteristic of N3 platinated 1-MeU. $[Pt_2Pd]^{2+}$ thus behaves similar to $[Pt_2Mn]^{2+}$, for which dissociation into its parent components had been observed before.[24] The difference in solution behavior to the oxidized species $[Pt_2Pd]^{3+}$ (vide infra) is noted.

Description of Crystal Structure of $[Pt_2Pd]^{2+}$. Figure 1 depicts the molecular cation of $[(NH_3)_2Pt(1\text{-}MeU)_2Pd(1\text{-}MeU)_2Pt(NH_3)_2](ClO_4)_2$, **3a**. Distances and angles about the metals are given in Table VI. The cation is centrosymmetric, consisting of two *cis*-$(NH_3)_2Pt^{II}$ moieties and one Pd^{II}, linked through four 1-MeU rings. Coordination of the two Pt atoms is through N3, of Pd via O4. All three metals adopt square-planar coordination geometries with no major deviations from planarity. Pt–Pd separations within the two crystallographically independent cations are 2.839 (1) and 2.837 (1) Å, which is shorter than in the dinuclear Pt–Pd complex **4a** (2.927 (1) Å)[18] but still substantially longer than in related $[Pt_2Mn]^{2+}$ (2.704 (1) Å)[24] and $[Pt_2Cu]^{2+}$ complexes (2.684 (1)[27] and 2.681 (1) Å[25]). The intermetallic distances in **3a** are close to that observed in $[Pt_2Ag]^+$ (2.866 (1) Å, av[17]), despite the differences in coordination geometries of the central metals in these complexes (distorted tetrahedral in $[Pt_2Ag]^+$, square-planar in **3a**). As a result of the relatively long Pt–Pd distances in **3a**, Pt and Pd coordination planes are substantially tilted (21.7°, 22.6°), slightly more than in $[Pt_2Mn]^{2+}$ (20.1°) and in $[Pt_2Cu]^{2+}$ (17.8[25] and 15.7° [27]). Pt–N distances compare well with values observed in a series of related compounds[24,25,27] Pd–O distances are similar to those observed in **4a**.[18] The 1-MeU rings are roughly at right angles to each other and planar as far as endocyclic atoms are concerned. There are no

---

(28) Schöllhorn, H.; Thewalt, U.; Lippert, B. *Inorg. Chim. Acta* **1985**, *108*, 77.

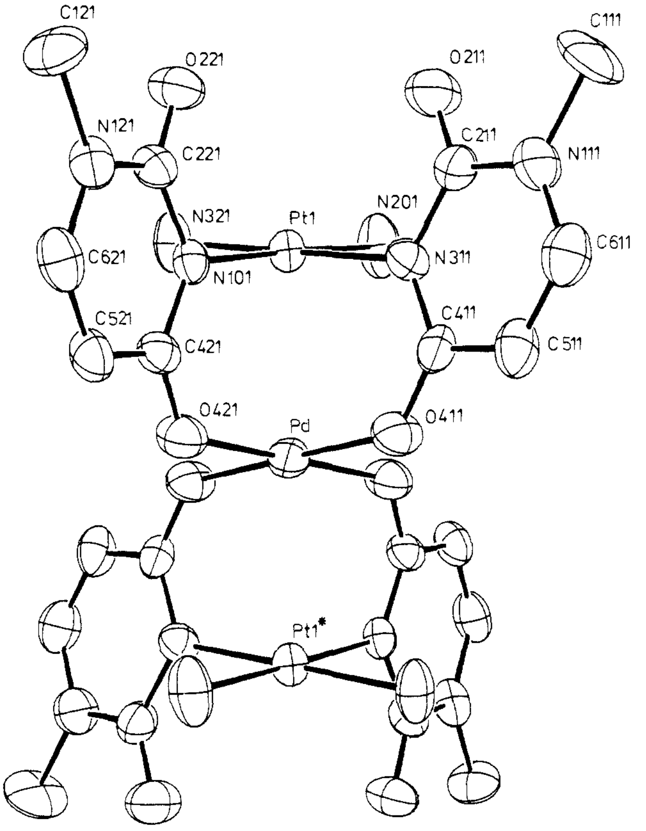

Figure 1. Molecular structure of one of the two crystallographically independent *cis*-$[(NH_3)_2Pt(1\text{-}MeU)_2Pd(1\text{-}MeU)_2Pt(NH_3)_2]^{2+}$ cations in **3a** (ORTEP plot, displacement parameters at the 50% probability level).

significant changes in bond lengths and angles when compared with related di- or trinuclear complexes of 1-MeU with N3,O4 metal coordination.

Chart II

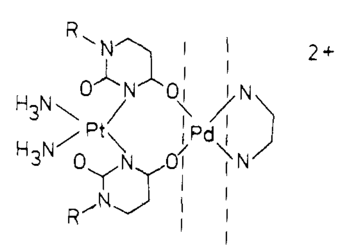

Table VI. Coordination Geometries about the Metals in **3a** (Distances in Å, Angles in deg) for Both Crystallographically Independent Molecules

(a) Pt Coordination Sphere	
Pt-N31	2.04 (1)/2.033 (8)
Pt-N32	2.035 (7)/2.034 (7)
Pt-N10	2.06 (1)/2.06 (1)
Pt-N20	2.068 (8)/2.058 (7)
Pt···Pd	2.839 (1)/2.837 (1)
N31-Pt-N32	90.2 (3)/89.0 (3)
N32-Pt-N10	87.8 (3)/89.7 (3)
N10-Pt-N20	93.0 (4)/91.1 (3)
N31-Pt-N20	89.0 (4)/90.3 (3)
N31-Pt-N10	177.7 (3)/178.6 (3)
N32-Pt-N20	178.4 (3)/179.1 (3)
(b) Pd Coordination Sphere	
Pd-O41	2.030 (9)/2.013 (8)
Pd-O42	2.036 (6)/2.017 (6)
O41-Pd-O42	88.6 (3)/91.0 (3)
O41-Pd-O42*	91.4 (3)/89.0 (3)
(c) Dihedral Angles	
Pt plane/Pd plane	21.7/22.6
Pt plane/1-MeU(1) plane	76.2/75.2
Pt plane/1-MeU(2) plane	85.5/85.6
1-MeU(1) plane/1-MeU(2) plane	103.8/98.6

$[Pt_2Pd]^{3+}$, 5. The oxidized form of **3** was obtained in three different ways as outlined below. Crystallization of the respective solutions gave different modifications of **5**, depending on concentration, pH, and anions present in solution. With 1-MeU as bridging ligands, the following compounds were isolated: $[(NH_3)_2Pt(1\text{-}MeU)_2Pd(1\text{-}MeU)_2Pt(NH_3)_2](NO_3)_3 \cdot HNO_3 \cdot 5H_2O$, **5a**; $[5](NO_3)_3 \cdot 11H_2O$, **5b**; $[5](NO_3)_3 \cdot 5H_2O$, **5c**; $[5](ClO_4)_3 \cdot 6H_2O$, **5d**. Substituting the *cis*-$(NH_3)_2$ ligands by ethylenediamine (en) and/or 1-MeU by 1-MeT gave three additional compounds: $[(en)Pt(1\text{-}MeU)_2Pd(1\text{-}MeU)_2Pt(en)](NO_3)_3 \cdot HNO_3 \cdot 6H_2O$, **5e**; $[(NH_3)_2Pt(1\text{-}MeT)_2Pd(1\text{-}MeT)_2Pt(NH_3)_2](NO_3)_3 \cdot 5H_2O$, **5f**; $[(en)Pt(1\text{-}MeT)_2Pd(1\text{-}MeT)_2Pt(en)](NO_3)_3 \cdot 12H_2O$, **5g**. Ways of preparations of **5** were as follows: (i) Oxidation of **3**. Addition of strong oxidants (Cl_2, concentrated HNO_3)[29] to aqueous solutions of **3** readily brought about oxidation according to

$$[Pt_2Pd]^{2+} \rightarrow [Pt_2Pd]^{3+} + e^-$$

Since this process is accompanied by a dramatic change in color from yellow-tan to deep blue, it was followed by UV-vis spectroscopy (Figure 2). For example, when **3** was dissolved in 1 M HNO_3 at 22 °C, formation of **5** had reached a maximum after 80 min (70% yield). (ii) Condensation of **1** and $[Pd(H_2O)_4]^{2+}$ in HNO_3. Addition of an aqueous, acidic (1.3 M HNO_3) solution of $[Pd(H_2O)_4](NO_3)_2$ to a solution of *cis*-$(NH_3)_2PtL_2$, **1**, led to a rapid color change from yellow via red to deep blue. On crystallization of the solution at 3 °C, **5** was obtained in 50% yield. We suspect that formation of **5** via this route involves the $[Pt_2Pd]^{2+}$ intermediate **3b** which, due to its rapid oxidation, is not isolated. (iii) HNO_3 Treatment of $[PtPd]^{2+}$, **4**. The dinuclear complex *cis*-$[(NH_3)_2Pt(1\text{-}MeU)_2Pd(en)](NO_3)_2$ aqueous, **4a**, which contains Pt bound to N3 and Pd coordinated via O4 (head-head),[18] undergoes a complicated rearrangement in HNO_3-acidic medium with partial formation of **5**, as evident from UV spectroscopy and confirmed by preparative results (**4b** → **5e**). In order to account for the formation of **5** from **4**, cleavage of the dinuclear complex **4** has to take place at the two positions indicated in Chart II. While the lability of O4-heterometal bonds,[31,32] and in particular with Pd^{II},[18] has been noted before, the cleavage of the enPd chelate certainly is remarkable. A feasible reaction scheme for the formation of **5** from **4** would be

$$2\underset{\mathbf{4}}{[A_2PtL_2Pd(en)]^{2+}} + 2H_3O^+ \rightarrow$$

$$\underset{\mathbf{3}}{[A_2PtL_2PdL_2PtA_2]^{2+}} + [(en)Pd(H_2O)_2]^{2+} + [enH_2]^{2}$$

and

$$3 \xrightarrow{\text{oxidation}} 5 \quad (A = NH_3 \text{ or } (en)/2)$$

Description of Crystal Structure of $[Pt_2Pd]^{3+}$. The crystal structures of the 1-MeU complexes **5a** and **5b** and of the 1-MeT complex **5g** were determined. Figures 3 and 4 show the cations of **5a** and **5g**. The cation of **5b** (not shown) is virtually identical with that of **5a**. Metal coordination spheres are presented in Table VII. Despite the apparent close similarities of these cations with that of **3a** in Figure 1—centrosymmetry, Pt coordination through N3, Pd coordination through O4, head-head orientation of the uracil (thymine) ligands—there are several major differences between **3a** and **5**. The first one refers to the charge. While the cation of **3a** has a +2 charge, the cations of **5** are tripositive. This charge results, at least formally from the presence of two metals

---

(29) Other oxidants used in nonpreparative experiments were $K_2S_2O_8$, $Ce(SO_4)_2$, and $H[AuCl_4]$.

(30) Neugebauer, D.; Lippert, B. *Inorg. Chim. Acta* **1982**, *67*, 151.

(31) Thewalt, U.; Neugebauer, D.; Lippert, B. *Inorg. Chem.* **1984**, *23*, 1713.

(32) Goodgame, D. M. L.; Hitchman, M. A.; Lippert, B. *Inorg. Chem.* **1986**, *25*, 2191.

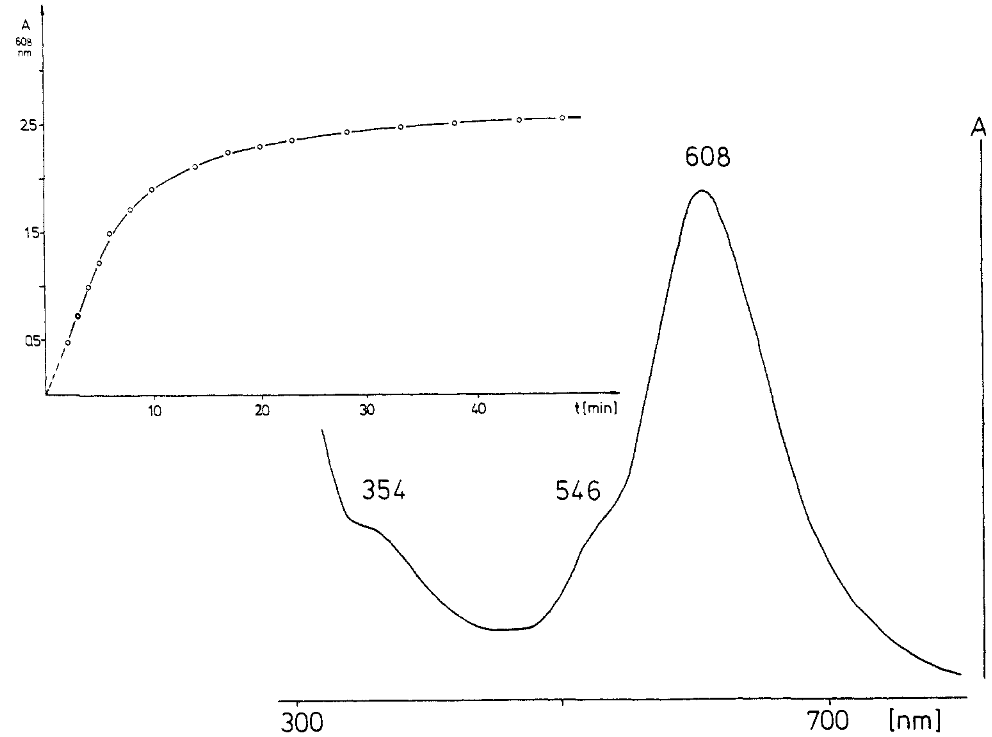

Figure 2. Visible spectra of $[Pt_2Pd]^{3+}$ (**5**) in HNO_3 and increase of 608-nm intensity (insert) as a function of time after dissolving $[Pt_2Pd]^{2+}$ (**3**) in 1 N HNO_3.

Table VII. Selected Interatomic Distances (Å) and Angles (deg) for $[(NH_3)_2Pt(1\text{-MeU})_2Pd(1\text{-MeU})_2Pt(NH_3)_2](NO_3)_3\cdot HNO_3\cdot 5H_2O$ (**5a**), $[(NH_3)_2Pt(1\text{-MeU})_2Pd(1\text{-MeU})_2Pt(NH_3)_2](NO_3)_3\cdot 11H_2O$ (**5b**), and $[(en)Pt(1\text{-MeT})_2Pd(1\text{-MeT})_2Pt(en)](NO_3)_3\cdot 12H_2O$ (**5g**)

	5a	**5b**	**5g**
(a) Pt Coordination Spheres			
Pt-N31	2.034 (7)	2.038 (8)	2.032 (4)
Pt-N32	2.025 (7)	2.027 (7)	2.032 (5)
Pt-N10	2.049 (7)	2.050 (7)	2.029 (4)
Pt-N20	2.043 (7)	2.052 (8)	2.015 (5)
Pt··Pd	2.634 (1)	2.641 (1)	2.646 (1)
N31-Pt-N32	89.5 (3)	92.0 (3)	90.8 (2)
N32-Pt-N10	89.6 (3)	89.1 (3)	92.4 (2)
N10-Pt-N20	90.5 (3)	88.6 (3)	83.2 (2)
N31-Pt-N20	90.4 (3)	90.3 (3)	93.7 (2)
N31-Pt-N10	178.9 (3)	179.0 (3)	176.6 (2)
N32-Pt-N20	178.9 (3)	177.7 (3)	175.5 (2)
(b) Pd Coordination Spheres			
Pd-O41	1.963 (7)	1.987 (6)	1.988 (3)
Pd-O42	1.998 (7)	1.998 (7)	1.992 (4)
O41-Pd-O42	90.6 (4)	88.9 (3)	90.9 (2)
O41-Pd-O42*	89.4 (4)	91.1 (3)	89.1 (2)
(c) Dihedral Angles^a			
Pt plane/Pd plane	14.5	15.4	16.2
Pt plane/L(1) plane	88.8	89.0	110.1
Pt plane/L(2) plane	78.1	69.9	84.8
L(1) plane/L(2) plane	82.5	87.4	95.6

^{a}L(1), L(2) = 1-MeU(1), 1-MeU(2) for **5a** and **5b** and 1-MeT(1), 1-MeT(2) for **5g**.

Table VIII. Absorptions in the Visible Spectra of $Pt_2^{II}Pd^{III}$ Complexes

λ (nm)	ε (M^{-1} cm^{-1})	solvent
(a) 1-MeU Compounds (**5a**, **5b** and **5e**)		
608	10850	0.1 N HNO_3
≃546	4180	
≃354	3350	
(b) 1-MeT Compound (**5g**)		
610	11200	0.7 N HNO_3
≃530	3580	
≃356	2940	

in the +II oxidation state and one metal in the +III oxidation state. Subtraction of four negative charges from the heterocyclic rings leaves a +3 charge. Certainly the most significant structural difference between **3a** and **5** is the shorter intermetallic distance in **5**—2.634 (1) Å in **5a**, 2.641 (1) Å in **5b**, and 2.646 (1) Å in **5g**—as a consequence of oxidation of **3** and subsequent metal-metal bonding in **5**. The shortening of the Pt-Pd distance of 0.20 Å (av), although quite significant, is relatively minor when compared with distances observed in $[Pt_2Mn]^{2+}$ and $[Pt_2Cu]^{2+}$ (see above), for which no strong metal-metal bond is assumed.[32] On the other hand, the difficulty in providing reliable values for metal-metal bond lengths is well known,[33] and even within a specific system (e.g., diplatinum(III) complexes with 1-MeU bridging ligands[34]) quite substantial differences due to effects of axial ligands are found. Another significant difference with respect to **3a** is the decrease in tilt angles between Pt and Pd coordination planes in **5**. The shortening of the intermetallic distance leads to a more parallel orientation of the planes. Values are 14.5° (**5a**), 15.4° (**5b**), and 16.2° (**5g**). A comparison of the bite distances of the uracil ligands (N3–O4 distance) in **3a** and **5a**, **5b**, and **5g** shows minor differences only (2.31 (1) Å in **3a**, 2.29 (1) Å in **5a**, 2.30 (1) Å in **5b** and **5g**), in agreement with the assumption that metal-metal bond formation rather than changes in ligand geometry is responsible for this effect. Finally, the significant shortening of Pd-O4 distances in **5** as compared to **3a** or the

---

[33] (a) O'Halloran, T. V.; Lippard, S. J. *Isr. J. Chem.* **1985**, *25*, 130 and references cited therein. (b) Woollins, J. D.; Kelly, P. F. *Coord. Chem. Rev.* **1985**, *65*, 115 and references cited therein. (c) Bancroft, D. P.; Cotton, F. A.; Falvello, L. R.; Schwotzer, W. *Inorg. Chem.* **1986**, *25*, 763 and references cited therein. (d) Goodgame, D. M. L.; Rollins, R. W.; Slawin, A. M. Z.; Williams, D. J.; Zard, P. W. *Inorg. Chim. Acta* **1986**, *120*, 91. (e) El-Mehdawi, R.; Fronczek, F. R.; Roundhill, D. M. *Inorg. Chem.* **1986**, *25*, 1155. (f) Che, C.-M.; Lee, W.-M.; Mak, T. C. W.; Gray, H. B. *J. Am. Chem. Soc.* **1986**, *108*, 4446. (g) Bellitto, C.; Bonamico, M.; Dessy, G.; Fares, V.; Flamini, A. *J. Chem. Soc., Dalton Trans* **1986**, 595.

[34] (a) Lippert, B.; Schöllhorn, H.; Thewalt, U. *J. Am. Chem. Soc.* **1986**, *108*, 525. (b) Schöllhorn, H.; Thewalt, U.; Lippert, B. *J. Chem. Soc., Chem. Commun.* **1986**, 258. (c) Schöllhorn, H.; Eisenmann, P.; Thewalt, U.; Lippert, B. *Inorg. Chem.* **1986**, *25*, 3384.

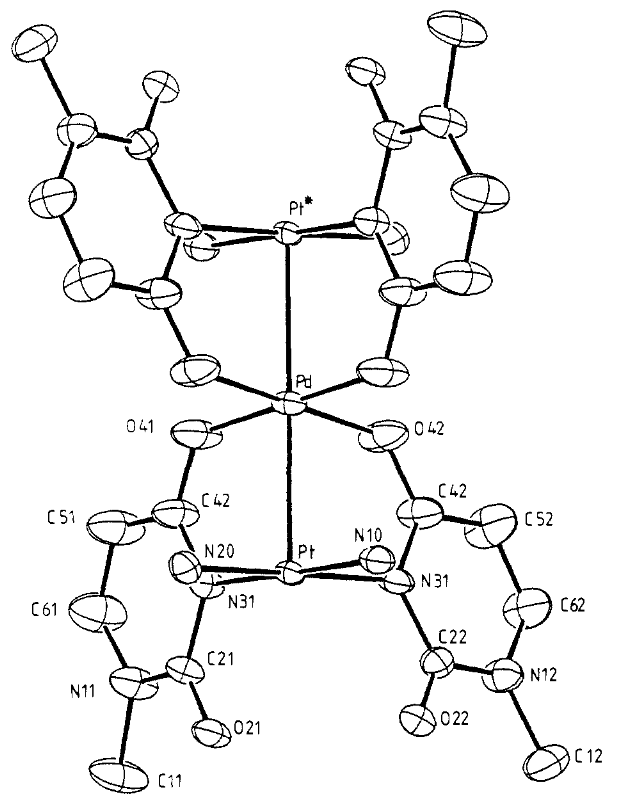

Figure 3. Molecular structure of the *cis*-$[(NH_3)_2Pt(1\text{-}MeU)_2Pd(1\text{-}MeU)_2Pt(NH_3)_2]^{3+}$ cation in **5a**. The cation of **5b** is virtually identical and is not shown.

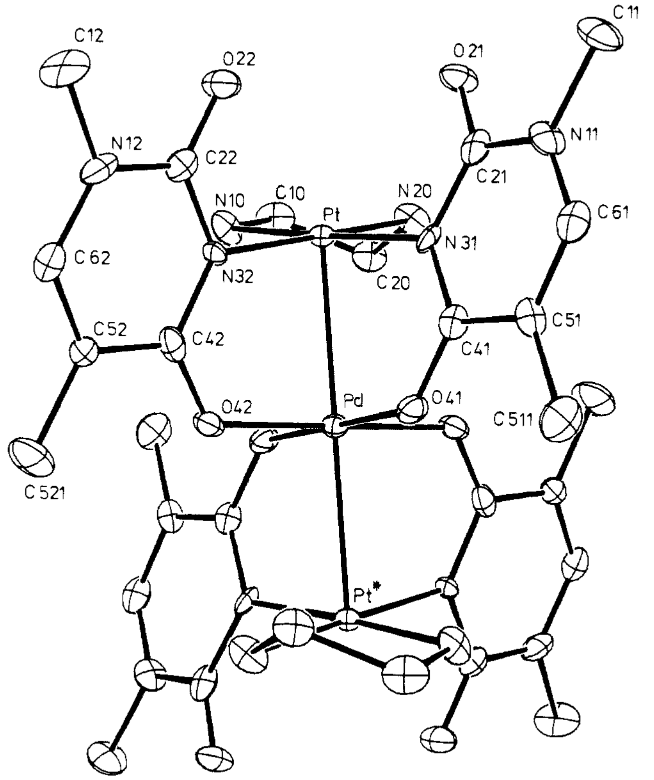

Figure 4. View of the $[(en)Pt(1\text{-}MeT)_2Pd(1\text{-}MeT)_2Pt(en)]^{3+}$ cation of **5g**.

related $[PtPd]^{2+}$ complex **4a** is noteworthy (2.024 Å av in **3a**, 1.988 Å av in **5a**, **5b**, and **5g**). It probably reflects the increase in oxidation state of Pd.

Table IX. Experimental Details and Results of Cyclic Voltammetric Studies with **5c**

	$[Pt_2Pd]^{4+}$/ $[Pt_2Pd]^{3+}$	$[Pt_2Pd]^{3+}$/ $[Pt_2Pd]^{2+}$	$[Pt_2Pd]^{2+}$/ $[Pt_2Pd]^{+}$
v [V s^{-1}]	0.005	0.400	0.005
E_{pc} [V]	1.288	0.620	−0.510
E_{pa} [V]	1.400	0.700	−0.340
ΔE_p [V]	0.120	0.080	0.170
$E_{1/2}$ [V]	1.340	0.0660	−0.425
D_o [cm^2 s^{-1}]	$1.5 \cdot 10^{-7}$	$1.5 \cdot 10^{-7}$	$1.5 \cdot 10^{-7}$
k_s^0 [cm s^{-1}]	$1.1 \cdot 10^{-4}$	$3.4 \cdot 10^{-3}$	$5.0 \cdot 10^{-5}$
$\Delta E_{p/2}$ (AC) [mV]	130	90	

As with **3a**, endocyclic atoms of 1-MeU and 1-MeT ligands in **5a**, **5b**, and **5g** do not show deviations from planarity of the rings. Unlike in the Pt(2.25) "blues" containing α-pyridonato ligands,[2,3] no capping interactions of counter ions and cations are observed in **3a** and in the three structures of **5**. The O2 oxygens of the 1-MeU (1-MeT) ligands protect the ends of the cations, thus preventing any close approach of anions.

Spectroscopy and Titration with Base. Crystals of all compounds **5** display metallic blue-purple lusters. Aqueous solutions of these complexes are deep blue due to strong absorptions around 608, 546, and 354 nm (1-MeU compounds) and 610, 530, and 356 nm (1-MeT compounds) (Table VIII). Variations of the amine ligands within one system (1-MeU or 1-MeT) have no significant effects on the spectra. In 0.1 N HNO_3, **5** is relatively stable as judged by the only slight decrease in absorbance with time (**5a**: 16% over a period of 18 h at room temperature). In contrast, Pt(2.25)-"blues" lose their green-blue color more rapidly.[8]

In the UV part of the spectrum, the strong $\pi \rightarrow \pi^*$ absorption of the 1-MeU ligand of **5a** is at 281 nm, suggesting that the trinuclear structure is retained even in dilute solution and that dissociation as observed for **3a** certainly is not significant. Thus metal–metal bond formation stabilizes the Pt_2Pd entity.

^1H NMR spectra of **5** (D_2O or DNO_3) do not display any resonances due to 1-MeU and 1-MeT ligands, respectively. Only in strongly alkaline solution (pD 11, sample yellow) are sharp resonances due to *cis*-A_2PtL_2 observed. Applying the NMR method of Evans,[35] magnetic moments of 1.89 μ_B for **5a** and 1.83 μ_B for **5g** were determined in DNO_3 acidic solutions. These values are consistent with the presence of one unpaired electron per trinuclear unit. EPR spectra of **5a** have been recorded in the solid state and in dilute solution. Qualitatively they are very similar to spectra obtained for "Pt blues". Details will be reported elsewhere.

As outlined in the crystallography section of the Experimental Section, proof of the presence of HNO_3 in **5a** is not fully straightforward. However, the strong similarity of the cation of **5a** with those of **5b** and **5g** and in particular the very similar Pt–Pd distances are indicative of identical oxidation states in all three structures. Moreover, the inclusion of acid in stoichiometric quantities in diplatinum(III) complexes is documented.[36] The pH of a solution of **5a** in water is, within experimental error, consistent with the presence of 1 HNO_3 per molecule. Titration of an aqueous solution of **5a** with NaOH exhibits the characteristics of titration of a strong acid (slow, linear increase in pH without buffer behavior). Unlike with pure HNO_3, the equivalence point is reached at pH 4.5 already due to superposition with a second neutralization process (possibly from $[Pd(H_2O)_x]^{n+}$) which is completed at pH 8.5–9.[37]

Redox Studies. The oxidative titration of **3** by Ce^{IV} (in 0.14 N HNO_3) was indicative of two processes: Initial oxidation of **3** to **5** with consumption of 1 equiv of Ce^{IV} per Pt_2Pd ($E°$ ca. 735 mV versus Ag/AgCl), as independently followed by visible spectroscopy (maximum intensity of 608-nm absorption reached at that point), and subsequent consumption of 2 additional equiv of Ce^{IV} per Pt_2Pd ($E°$ ca. 937 mV versus Ag/AgCl). The intensity of the 608-nm band decreases only slightly during this process (cf. Supplementary Material). The nature of this second oxidation

---

(35) Evans, D. F. *J. Chem. Soc.* **1959**, 2003.

(36) See, e.g.: (a) Reference 33e. (b) Reference 34b.

(37) In a related system (ref 34b), we have conclusively found that this method of potentiometric titration is capable of determining the exact amount of acid present. Details will be published shortly.

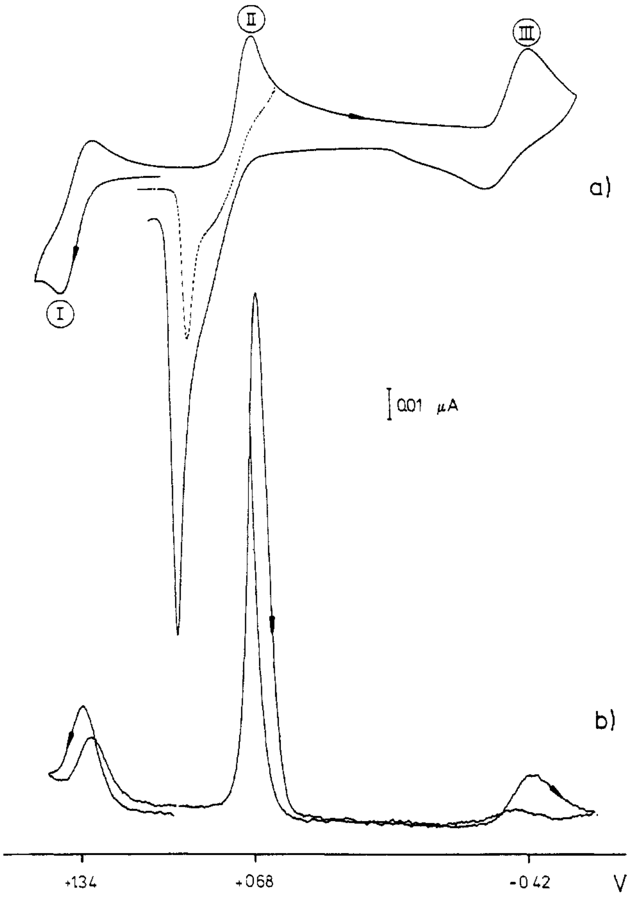

Figure 5. Cyclic voltammogram (a) and ac voltammogram (b) of **5c** in the range $-0.72 \leqslant E\ [V] \leqslant +1.50$.

step is unclear at present, especially since it is not consistent with the cyclovoltammetry data obtained in propylenecarbonate.

Figure 5 depicts the cyclic dc and ac voltammograms of **5c** in the range between −0.72 and +1.50 V. Propylenecarbonate was used to avoid follow-up reactions at a higher oxidation level. Due to insufficient solubility, the $[Pt_2Pd]^{2+}$ species could not be applied. The voltammograms in Figure 5 indicate the existence of four interconvertible redox states

$$[Pt_2Pd]^{+} \overset{E^\circ = -0.425\ V}{\rightleftharpoons} \underset{\mathbf{3}}{[Pt_2Pd]^{2+}} \overset{E^\circ = +0.68\ V}{\rightleftharpoons} \underset{\mathbf{5}}{[Pt_2Pd]^{3+}} \overset{E^\circ = +1.34\ V}{\rightleftharpoons} [Pt_2Pd]^{4+}$$

All three electron-transfer processes are electrochemically quasi-reversible (Table IX) with heterogeneous rate constants between $k_s{}^\circ = 10^{-3}$ and 10^{-5} cm s^{-1} as documented by the ΔE_p separations and the peak current heights in the dc and ac experiments. As all half-height widths in the ac voltammograms lie between 90 and 130 mV, the redox steps are uniformly one-electron-transfer reactions. In addition to the chemically almost reversible redox reactions, an irreversible process takes place at $E_p = +1.90$ V, which probably causes destruction of the complex.

The oxidation of $[Pt_2Pd]^{3+}$ to $[Pt_2Pd]^{4+}$ (wave I) is followed by a slow chemical secondary reaction. This is evident both from the current function $i_{pa}/v^{1/2}$ and from the peak current ratio i_{pc}/i_{pa}, which decreases and increases, respectively, with increasing scan rate. The redox couple $[Pt_2Pd]^{3+}/[Pt_2Pd]^{2+}$ has its standard potential at $E^\circ = 0.670$ V (wave II). This value compares reasonably well with the value obtained in water (see above). Its heterogeneous charge transfer is significantly faster than in the case of the $[Pt_2Pd]^{4+}/[Pt_2Pd]^{3+}$ couple. However, as can be seen from Figure 5, the reoxidation step is accompanied by a strong adsorption process which was also observed during the oxidative titration of **3** with Ce^{IV}. The adsorption is minimized when the cathodic switching potential during the CV experiment is close to the standard redox potential of the $[Pt_2Pd]^{3+}/[Pt_2Pd]^{2+}$ couple (Figure 6). The third redox process leading to $[Pt_2Pd]^+$ is observed at $E^\circ = -0.425$ V (versus Ag/AgCl). Its heterogeneous kinetics are sluggish. All three redox states display extremely low diffusion coefficients D_0 of ca. $1.5 \cdot 10^{-7}$ cm^2 s^{-1}.

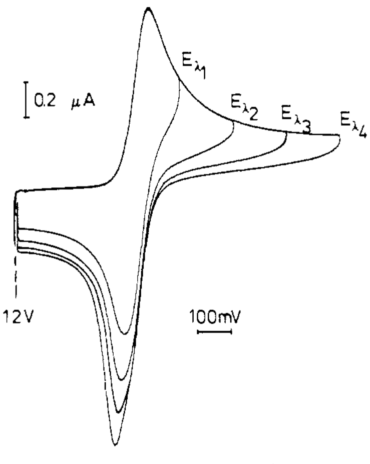

Figure 6. Cyclic voltammograms of $[Pt_2Pd]^{3+}/[Pt_2Pd]^{2+}$ couple as a function of the switching potential E_λ.

The accurate description, viz. distribution of formal oxidation states for the three metals in $[Pt_2Pd]^{n+}$ (n = 1, 2, 3, 4), is unambiguous for n = 2 only, with all three metals being in the +II state. As mentioned above, for n = 3 the crystallographic data (shortening of Pd–O4 bonds) and EPR spectra[10] seem to suggest that **5** is close to $Pt^{II}{}_2Pd^{III}$. Despite all differences in ligand nature, the E° value of the **3**/**5** couple is in the range of that of a mononuclear Pd^{III} complex containing two 1,4,7-trithiacyclononane ligands.[38] Using similar arguments for the $[Pt_2Pd]^+$ species, it would seem that the much more negative potential for the reduction of a Pd^{II} complex containing a tetraazamacrocycle to the corresponding Pd^I species[39] rules against a $Pt^{II}{}_2Pd^I$ formalism. As to $[Pt_2Pd]^{4+}$, despite the documented existence of Pd^{IV} in mononuclear and linear chain complexes,[40] the correct formulation is unclear at present. It is noted, that in a linear Rh$_3$ complex a similar $d^8d^6d^8$ system is realized,[41] but ligand oxidation as recently observed in a dinuclear Pd complex[42] cannot be fully ruled out at this point.

Summary. In this work, the synthesis, crystal structures, and solution studies of linear, trinuclear PtPdPt complexes containing bridging 1-MeT and 1-MeU nucleobases is reported. As indicated by cyclovoltammetry experiments, the trinuclear cations can exist in four different combinations of metal oxidation states. Two of them, $Pt^{II}{}_2Pd^{II}$ and $Pt^{II}{}_2Pd^{III}$, have been isolated and structurally characterized. $Pt^{II}{}_2Pd^{III}$, which is paramagnetic and intensely purple-blue, is considered a model of a trinuclear "Pt pyrimidine blue" with an average 2.33 metal oxidation state.

Acknowledgment. This work has been supported by the Deutsche Forschungsgemeinschaft, the Fonds der Chemischen Industrie, and Degussa (loan of K_2PtCl_4).

Supplementary Material Available: Graph of oxidative titration of $[Pt_2Pd]^{2+}$ and complete tables of atomic coordinates and anisotropic displacement parameters for **3a**, **5a**, **5b**, and **5g** (22 pages); tables of observed and calculated structure factors (91 pages). Ordering information is given on any current masthead page.

---

[38] Blake, A. J.; Holder, A. J.; Hyde, T. I.; Schröder, M. *J. Chem. Soc., Chem. Commun.* **1987**, 897.

[39] Blake, A. J.; Gould, R. O.; Hyde, T. I.; Schröder, M. *J. Chem. Soc., Chem. Commun.* **1987**, 431.

[40] See, e.g.: (a) Byers, P. K.; Canty, A. J.; Skelton, B. W.; White, A. H. *J. Chem. Soc., Chem. Commun.* **1987**, 1093. (b) Toriuma, K.; Yamashita, M.; Ito, H.; Ito, T. *Acta Crystallogr., Sect. C: Cryst. Struct. Commun.* **1986**, *C42*, 963. (c) Clark, R. J.; Trumble, W. R. *Inorg. Chem.* **1976**, *15*, 1030.

[41] Balch, A. L.; Olmstead, M. M. *J. Am. Chem. Soc.* **1979**, *101*, 3128.

[42] Cotton, F. A.; Matusz, M.; Poli, R.; Feng, X. *J. Am. Chem. Soc.* **1988**, *110*, 1144.